IEEE Photonics Journal
An IEEE Photonics Society Publication

Open Access

Reconfigurable Rectangular Filter With Continuously Tunable Bandwidth and Wavelength

Volume 12, Number 4, August 2020

Jiachen Li
Sigang Yang, *Member, IEEE*
Hongwei Chen, *Member, IEEE*
Minghua Chen, *Member, IEEE*

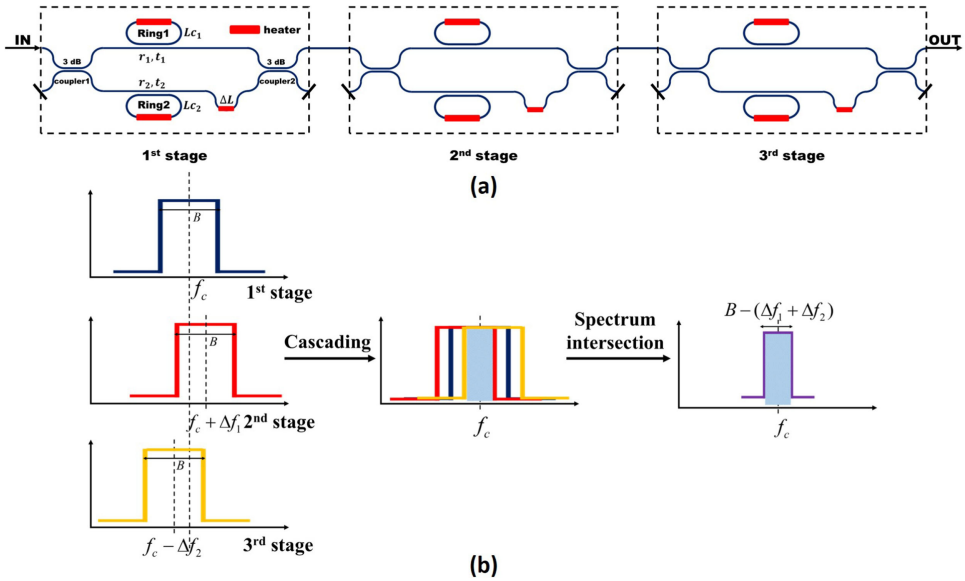

DOI: 10.1109/JPHOT.2020.3003787

Reconfigurable Rectangular Filter With Continuously Tunable Bandwidth and Wavelength

Jiachen Li,[1,2] **Sigang Yang**,[1,2] ***Member, IEEE***,
Hongwei Chen,[1,2] ***Member, IEEE***,
and Minghua Chen,[1,2] ***Member, IEEE***

[1]Department of Electronic Engineering, Tsinghua University, Beijing 100084, China
[2]Beijing National Research Center for Information Science and Technology (BNRist), Beijing 100084, China

DOI:10.1109/JPHOT.2020.3003787

Manuscript received May 22, 2020; revised June 11, 2020; accepted June 15, 2020. Date of publication June 19, 2020; date of current version June 30, 2020. This work was supported in part by the National Natural Science Foundation of China under Contract 61771285 and in part by the National Key Research and Development Program of China under Contract 2018YFB2201802. Corresponding author: Minghua Chen. (e-mail: chenmh@tsinghua.edu.cn).

Abstract: We propose and demonstrate a rectangular optical lattice filter with reconfigurable bandwidth and wavelength. The proposed reconfigurable rectangular lattice filter consists of three-stage cascaded ring-assisted Mach-Zehnder interferometers (RAMZIs), and each RAMZI unit serves as an approximate optical elliptical filter with optimized shape factor. The scheme and design principle are presented with the method of zero-pole theory. As a proof of concept, the proposed structure is fabricated on the Si_3 N_4 waveguide platform. In the experiment, the 3-dB bandwidth of the proposed filter can be continuously tuned from 14.1 GHz to 4.1 GHz, maintaining a rectangular transmission response, and the wavelength can also be continuously tuned. This reconfigurable rectangular optical lattice filter shows the potential in many practical applications for reconfigurable optical signal processing due to flexibility and reconfigurability.

Index Terms: Integrated photonics, waveguide devices, tunable filters, optical signal processing.

1. Introduction

The reconfigurability of optical filters is an essential capability, enabling adaption to data rate variation and dynamic changes [1]–[3], as optical transport networks evolve to be more flexible to increase the communication capacity. Besides, reconfigurable optical filters are of great significance for microwave photonics to realize large-range reconfigurable microwave signal processing [4]. Typically, the reconfigurable rectangular optical filter is especially valuable in practical applications for its unique advantages, including flexible frequency selectivity, good shape factor, and large out-band suppression [1]. For example, in multiband orthogonal frequency-division multiplexing (MB-OFDM) system, an optical filter with a tunable 3-dB bandwidth from 14 GHz to 4 GHz is a crucial device to realize the add-drop function for the variable bit rate. Moreover, the transmission response of the employed filter is required to be as rectangular as possible to reduce the distortion to neighboring sub-bands [3].

Previous approaches to demonstrate such a reconfigurable rectangular filter can be broadly classified into two categories. The first method is summarized as spectrum combination, which means that the spectral response is the combination of all units, and the output bandwidth can be adjusted by separately tuning wavelength spacings between different units. Typical schemes include multi-microring structure [5]–[7], ring-assisted Mach-Zehnder interferometer (RAMZI) [8]–[10], and microring-MZI structure [11]. However, the employed unit filter for the spectrum combination method is usually microring resonator, leading to the limited bandwidth tuning range. Besides, the insertion loss and the rectangular spectral response usually vary dramatically during the bandwidth reconfiguration. Therefore, the spectrum combination method cannot meet our requirement for a stable rectangular response with a broad bandwidth tuning range. The second method is spectrum intersection, implying that the equivalent spectral response is the intersection of transmission responses of all units, and the bandwidth is decided by the scale of the overlapping span. For example, an optical lattice filter [12], consisting of two-stage cascaded grating filters, is employed to generate a bandwidth-tunable rectangular response [13]. For the spectrum intersection method, a rectangular unit filter with a low shape factor ($SF_{10\,dB}$, defined as the ratio of bandwidth at 10 dB to 3 dB) and a flat passband is essential to guarantee the rectangular transmission response and the stable insertion loss during the bandwidth reconfiguration, which are the most important advantages of the spectrum intersection method, compared with the spectrum combination method. In addition to the two approaches mentioned above, there are other alternative solutions, such as stimulated Brillouin scattering (SBS) technique [14] and multi-tap MZI [15]. However, they are difficult to be implemented on the integrated platform, and their control is complex. In summary, compared with the spectrum combination and other solutions, the method of spectrum intersection is a reasonable choice for demonstrating a reconfigurable rectangular filter with a broad bandwidth tuning range on the integrated photonics platform.

In this paper, we propose and demonstrate a rectangular optical lattice filter with a reconfigurable bandwidth, based on the spectrum intersection method. The proposed optical lattice filter consists of three-stage cascaded RAMZIs, and each RAMZI unit filter is optimized to approximate an optical elliptic filter with good shape factor. The principle is explained with the method of zero-pole theory in detail. The device is demonstrated on the double-strip Si_3 N_4 platform. With micro heaters for the initial calibration and accurate control, the 3-dB bandwidth of the lattice filter can be tuned continuously from 14.1 GHz to 4.1 GHz, maintaining the good shape factor and the low insertion loss. With these advantages, the proposed reconfigurable rectangular filter shows great potential for various applications, such as reconfigurable microwave photonic RF frontend [4] and modern optic communication [3].

2. Principle and Simulation Results

Fig. 1(a) shows the structural diagram of the reconfigurable optical lattice filter based on three-stage cascaded RAMZIs. Each RAMZI, consisting of an asymmetric MZI and two microring resonators placed on two arms of the MZI [16], is optimized to approximate an optical rectangular filter unit with a low shape factor, and three micro heaters are introduced for tuning the wavelength and compensating fabrication errors utilizing thermo-optic effect. With this optimized RAMZI filter unit, a rectangular lattice filter with a variable bandwidth can be achieved using the spectrum intersection method, and its basic principle is interpreted in Fig. 1(b). When the center wavelengths of three stages are tuned to be different, only the overlapping passbands of three RAMZI units make contributions to the overall output. Hence, the bandwidth of the proposed lattice filter can be adjusted by tuning the scale of the overlapping span. As is shown in Fig. 1(b), the bandwidth of the lattice filter is indicated as $B - (\Delta f_1 + \Delta f_2)$, where B is the intrinsic bandwidth of each RAMZI unit, Δf_1 and Δf_2 are frequency offsets between three stages. Besides, compared with the traditional two-stage structure for the spectrum intersection, the employed three-stage structure can enlarge the sideband suppression ratio and the free spectral range (FSR) of the rectangular lattice filter [17].

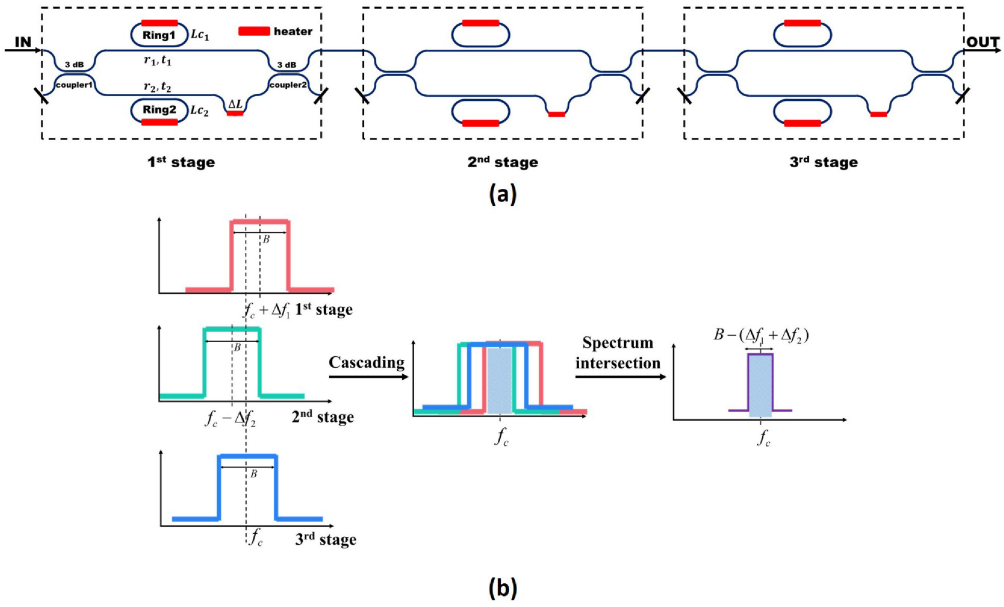

Fig. 1. (a) Structural diagram of the proposed rectangular lattice filter consisting of three-stage cascaded RAMZIs. (b) Schematic principle of the employed spectrum intersection method.

We optimize each RAMZI unit filter to approximate a rectangular digital filter with the method of zero-pole theory. Among classical digital filters, the elliptic filter shows narrower transition bandwidth with the same order [18], resulting in a better shape factor, compared with Chebyshev filters [19] and Butterworth filters [7]. Therefore, we choose to achieve an approximate optical elliptic filter by optimizing parameters of the RAMZI [20], [21], so we can simultaneously obtain a flat passband and a sharp edge steepness. As is shown in the first-stage RAMZI in Fig. 1(a), Lc_1 and Lc_2 are perimeters of two microrings, and ΔL is the length difference between two arms of the MZI. Besides, r_1 and r_2 are field self-coupling coefficients of two microrings. Therefore, with the method of transfer matrix [22], the transfer function of a single-stage RAMZI is expressed as:

$$H_{RAMZI}(\beta) = \frac{1}{2}\left(\frac{r_1 + e^{-j(\beta - j\alpha)Lc_1}}{1 + r_1 e^{-j(\beta - j\alpha)Lc_1}} - \frac{r_2 + e^{-j(\beta - j\alpha)Lc_2}}{1 + r_2 e^{-j(\beta - j\alpha)Lc_2}} e^{-j(\beta - j\alpha)\Delta L}\right), \tag{1}$$

where $\beta = 2\pi n/\lambda$ represents the propagation coefficient and α represents the amplitude attenuation coefficient of the employed waveguide platform. Assuming $Lc_1 = Lc_2 = 2\Delta L$, based on the theory of digital filter [22], equation (1) can be rewritten as:

$$\begin{aligned} H_{RAMZI}(z) &= \frac{1}{2}\left(\frac{r_1 + a^2 z^{-2}}{1 + r_1 a^2 z^{-2}} - \frac{r_2 + a^2 z^{-2}}{1 + r_2 a^2 z^{-2}} z^{-1}\right) \\ &= \frac{1}{2}\frac{r_1 - r_2 a z^{-1} + (r_1 r_2 + 1)a^2 z^{-2} - (r_1 r_2 + 1)a^2 z^{-3} + r_2 a^4 z^{-4} - r_1 a^5 z^{-5}}{1 + (r_1 + r_2)a^2 z^{-2} + r_1 r_2 a^4 z^{-4}} \\ &= \frac{\sum_{r=0}^{5} b_r z^{-r}}{1 + \sum_{k=1}^{4} a_k z^{-k}}. \end{aligned} \tag{2}$$

Here, $a^2 = e^{-\alpha 2\Delta L}$ represents the round-trip amplitude attenuation coefficient of the microring resonator, and $z^{-2} = e^{-j\beta 2\Delta L}$ represents the round-trip phase coefficient of the microring resonator. From equation (2), the RAMZI filter is equivalent to a five-order digital filter with five zeros and five poles (one pole is fixed at the origin). The locations of zeros and poles are decided by field

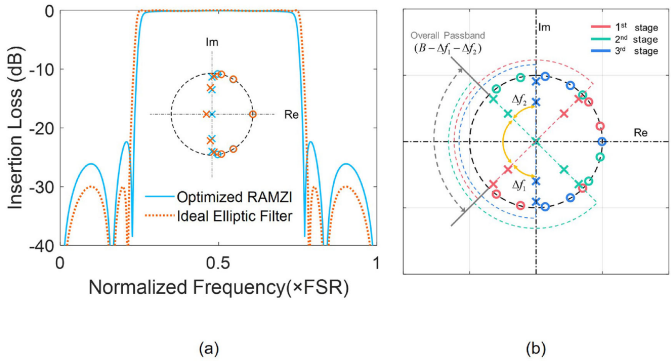

(a) (b)

Fig. 2. (a) Spectral responses and zero-pole graphs of the desired five-order elliptic filter and the optimized RAMZI ($r_1 = 0.361$, $r_2 = 0.837$). (b) Zero-pole graph of the reconfigurable lattice filter based on three-stage optimized RAMZI units, with the method of the spectrum intersection. Zeros (circles), poles (crosses), and passbands (semicircles with dotted line) of three stages are marked with different colors.

self-coupling coefficients of two microrings (r_1 and r_2) and the attenuation coefficient (a). With the commercial digital filter design tool (MATLAB Filter Designer [23]), we automatically generate the zeros and poles of an ideal five-order elliptic filter, as shown in the inset of Fig. 2(a). Considering that the five zeros of the elliptic filter are located on the unit circle in the complex z-plane, the transmission attenuation coefficient α is required to be as small as possible (0.1 dB/cm in our simulation), for a better approximation (a$\approx$ 1) to the generated elliptic filter. Then the field self-coupling coefficients of two microrings can be inversely solved by fitting the zeros and poles. However, limited by the overdetermined equations, the zeros and poles of the RAMZI cannot completely coincide with those of the desired five-order elliptic filter. Hence, the least-square method is utilized to achieve the approximation, and r_1 and r_2 are determined to be 0.361 and 0.837, separately. The zero-pole graph and the spectral response of the approximate RAMZI-based elliptic filter are shown in Fig. 2(a). From simulation results, the shape factor of the optimized RAMZI filter is 1.07 and the sideband suppression ratio is more than 20 dB, which agree well with the desired elliptic filter.

With such optimized RAMZI unit mentioned above, a rectangular optical lattice filter with a tunable bandwidth can be achieved with the method of spectrum intersection, and the three-stage cascaded structure is used to enlarge the sideband suppression ratio which decreases due to the approximation and fabrication errors. The transfer function of such a lattice filter based on three-stage cascaded RAMZIs can be expressed as:

$$H_{three-stage} = H_{RAMZI}(z_1)H_{RAMZI}(z_2)H_{RAMZI}(z_3). \tag{3}$$

The principle of the employed spectrum intersection method is explained with the zero-pole theory as well. As illustrated in Fig. 2(b), the three-stage cascaded lattice filter owns fifteen zeros and fifteen poles (three of them are at the same location), provided by three different RAMZI units. Propagation coefficients of three stages differ from each other due to different phase tunings, which means that the zeros and poles of each stage rotate a certain angle from the initial state, resulting in the rotation of the corresponding passband along the unit circle in the z-plane. Therefore, we can change the bandwidth by controlling the angle that each stage rotates. In Fig. 2(b), zeros and poles of three stages are marked with different colors, and semicircles (dotted lines) with corresponding colors represent passbands of three RAMZIs. Moreover, with all the zeros and poles of three stages rotating the same angle along the unit circle as a whole, the center wavelength of the lattice filter can be arbitrarily tuned within one FSR.

As is shown in Fig. 3, we plot the simulated transmission spectra of the rectangular optical lattice filter with a tunable bandwidth and center wavelength. In Fig. 3(a), the 3-dB bandwidth can be continuously tuned from 0.488 FSR to 0.049 FSR, maintaining a stable rectangular response with

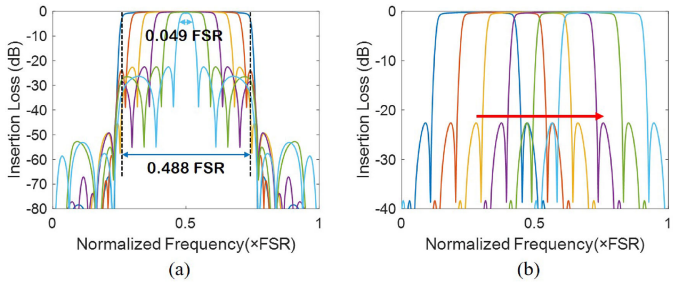

Fig. 3. (a) The bandwidth of the proposed lattice filter can be continuously tuned from 0.488 FSR to 0.049 FSR, maintaining good rectangular spectrum response, and the extinction ratio keeps more than 20 dB. (b) The wavelength of the lattice filter can be adjusted arbitrarily within one FSR.

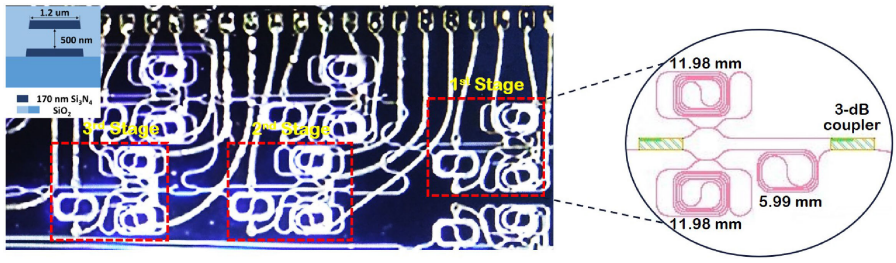

Fig. 4. Micrograph of the fabricated Si_3N_4 photonic integrated circuit. Inset is the cross section of the waveguide.

good sideband suppression ratio (>20 dB) and negligible insertion loss (about 0.1 dB with $\Delta L = 5990\ \mu$m and $\alpha = 0.1$ dB/cm). Obviously, for the employed spectrum intersection method, the upper limit of the output bandwidth equals the intrinsic bandwidth of the optimized RAMZI unit. In contrast, the lower limit is decided by the transition bandwidth of the RAMZI, which brings forward a higher requirement for the shape factor of the RAMZI unit. Expressly, the minimum passband is limited by bandwidths of the rising edge and the falling edge of the rectangular spectral response of each stage. In Fig. 3(b), the simulation indicates that the center wavelength of the proposed rectangular lattice filter can be arbitrarily adjusted within one FSR.

3. Device Fabrication and Experimental Results

The proposed rectangular optical lattice filter is demonstrated on the TriPleX double-strip Si_3N_4 waveguide platform with a low loss of about 0.1 dB/cm [24]. The low-loss Si_3N_4 waveguide helps to obtain a more accurate approximation to the desired elliptic filter (see Fig. 2(a)) and allows a longer ΔL between two arms of the RAMZI unit for a narrower minimum bandwidth, which is proportional to the FSR (see Fig. 3(a)). Besides, Si_3N_4 owns a wide optical window, which is another important advantage for the optical filter. In our demonstration, the length difference ΔL between two arms of the RAMZI is designed to 5990 μm to achieve an FSR of 32 GHz, and the circumference of the microring resonator is twice that. Based on the simulation via the three-dimensional finite-difference time-domain (3D-FDTD) method, the coupling gaps of two microrings in the optimized RAMZI unit are 1.1 μm (longer arm) and 1.0 μm (shorter arm), respectively, with the same coupling length of 88 μm. Besides, Cr-Au metal heaters are formed to realize the phase tuning utilizing the thermo-optic effect. The micrograph of the fabricated device is shown in Fig. 4.

Due to unavoidable fabrication errors, including deviations of the waveguide with and the waveguide length, the calibration process is a necessary operation before the experiment. By applying different voltages on heaters, we can tune the effective refractive index of different

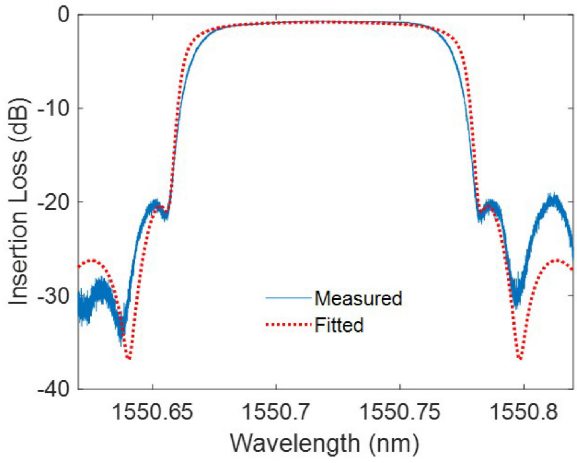

Fig. 5. The reconstructed spectral response of the first stage and its corresponding simulation.

parts to compensate imperfections caused by the manufacturing process. However, it is complex to simultaneously control nine micro heaters of three stages for the calibration. A simple but practicable solution is calibrating parameters stage by stage. Firstly, we reconstruct the spectral response of the first stage based on all the outputs of the other two stages, and the three heaters of the first stage are calibrated by fitting the spectral response to the optimized RAMZI unit. Then, the same calibration method is implemented as mentioned before for the next two stages. Therefore, the whole calibration process is divided into three steps for reducing the complexity, and each is equivalent to calibrating a single-stage RAMZI. After calibration, the voltages applied on the nine micro heaters had unequal initial values ranging from 2.2 V to 6.8 V, which means the power consumption is from 32 mW to 308 mW with the heater resistance of 150 Ω.

We measure transmission spectral responses of the fabricated device by employing an advanced optical spectrum analyzer (APEX, AP2081B) with a built-in tunable laser, and its measurement accuracy reaches 20 MHz. In the experiment, two PM fiber arrays are coupled with the fabricated device to avoid the extra insertion loss caused by the polarization, and a low coupling loss of less than 2 dB per facet for the TE polarization can be achieved with the spot size converter [24] offered by the LioniX. However, for TM polarization, the coupling loss is more than 20 dB per facet. Thus, the fabricated device is polarization-insensitive. Besides, a thermoelectric cooler was placed under the device to suppress the wavelength drift caused by the temperature variation, which is about 15 pm/K for the employed waveguide platform [25].

To illustrate the performance of the optimized RAMZI unit, we reconstruct the spectral response of the first-stage RAMZI and fit it to the theoretical model based on equation (1). The reconstructed spectral response and its corresponding simulation are plotted in Fig. 5. The shape factor is 1.2, the intrinsic insertion loss is about 1.2 dB, and the extinction ratio (ER) is about 20 dB, which are not as good as the simulation results shown in Fig. 2(a). That is mainly because the coupling coefficients of two microrings and the waveguide loss in the fabricated device deviate from our design values. According to the fit of model, the coupling coefficients are 0.38 (r_1) and 0.86 (r_2), and the waveguide loss is about 0.45 dB/cm. Because the transition bandwidth becomes wider than the simulation in Fig. 2(a), the reconfigurable minimum bandwidth cannot reach 0.049 FSR. Besides, the extinction ratio is also influenced during the bandwidth reconfiguration to some extent.

We demonstrate the bandwidth reconfigurability of the rectangular lattice filter by changing the scale of overlapping passbands of three stages, with different heating power applied on micro heaters after calibration. As is shown in Fig. 6(a), the 3-dB bandwidth can be continuously tuned from 14.1 GHz to 4.1 GHz with the measured FSR of 29.2 GHz. Besides, the insertion loss (IL) of the fabricated device maintains about 7 dB during bandwidth reconfiguration, which includes the

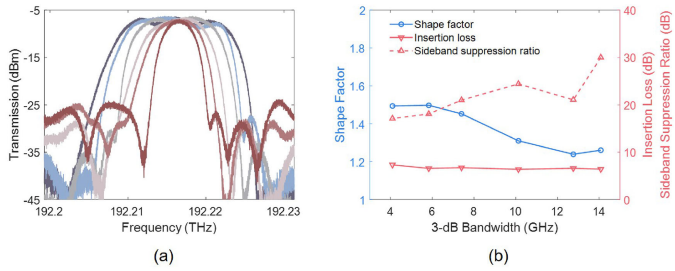

Fig. 6. (a) Measured transmission responses with tunable 3-dB bandwidths. (b) The shape factor, the sideband suppression ratio, and the insertion loss vary with different 3-dB bandwidths.

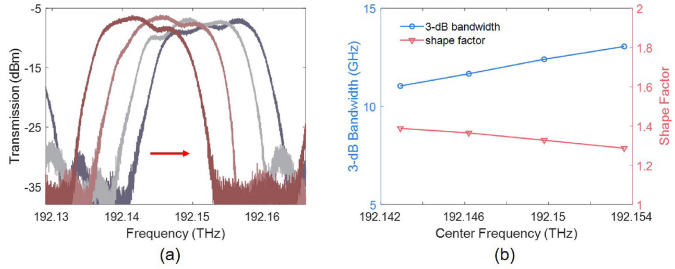

Fig. 7. (a) Measured transmission responses with tunable center frequency. (b) The shape factor and the 3-dB bandwidth vary slightly with the center frequency.

TABLE 1
Performance Comparisons of Different Integrated Bandwidth-Tunable Rectangular Filters

Literature	Scheme	3-dB bandwidth	SF	IL (dB)	ER (dB)	Response
This work	Three-stage cascaded RAMZIs	14.1-4.1 GHz	1.239-1.497	3-4	30-17.1	stable
[5]	Second-order microring	80-7 GHz	1.5-3	NA	14.4-11.15	not stable
[6]	Multiple-microring-based Vernier filter	1.2-0.3 nm	1.5-2.5	5.5-1.7	10-16.3	not stable
[8]	Single-stage RAMZI (four rings)	2.4-0.8 GHz	1.3-1.7	3-6	>25	stable
[11]	Microring-MZI	0.88-0.46 nm	1.5	>6	30	stable

coupling loss of two facets. Thus, the intrinsic insertion loss of the lattice filter is less than 4 dB. From Fig. 6(b), with the 3-dB bandwidth tuned from 14.1 GHz to 4.1 GHz, the sideband suppression ratio gradually reduces from 30 dB to 17.1 dB, and the shape factor increases from 1.239 to 1.497. Moreover, the insertion loss varies less than 1 dB with different bandwidths. Therefore, the experimental results of the bandwidth tunability are consistent with the simulation. However, due to the imperfect tuning process and fabrication errors of coupling coefficients as mentioned above, the lower limit of the 3-dB bandwidth and the sideband suppression ratio are slightly different from the simulation.

We demonstrate the wavelength tunability of the rectangular lattice filter as well, and the results are shown in Fig. 7. The center frequency is tuned from 192.143 THz to 192.154 THz by applying the same frequency tuning on three stages, as a proof of concept. As shown in Fig. 7(b), with the tuning of center frequency, the shape factor gradually varies from 1.39 to 1.29, and the 3-dB bandwidth changes from 11 GHz to 13 GHz. Hence, the center frequency can be adjusted without changing the shape factor and the bandwidth, basically. The slight variation of the transmission response is caused by different adjustments of three stages, which is caused by the thermal crosstalk between different micro heaters, This problem can be further improved by using an automatic control algorithm with developing the thermal crosstalk matrix model [26].

In Table 1, we summarize the performances of different schemes for a bandwidth-tunable rectangular filter. Compared with other listed methods, the proposed lattice filter based on three-stage cascaded RAMZIs features essential advantages of the low shape factor and the stable rectangular filter response. On the one hand, the measured low shape factor (1.239-1.497) shows that the transmission response is more rectangular than the multi-ring structure with a shape factor larger than 1.5 [5], [6], which is the commonly-used structure to achieve the rectangular transmission response. On the other hand, the proposed lattice filter shows a stable rectangular filter response (see Fig. 6(a)) with consistent insertion loss, shape factor, and extinction ratio. Therefore, these two important advantages make the proposed structure more attractive in reconfigurable analog optical signal processing.

However, as shown in experimental results, some performances can be further improved. First, the fabrication errors result in the worsening sideband suppression ratio and the larger shape factor of the RAMZI unit, as shown in Fig. 5. Therefore, we can optimize the design of microring coupling gaps. Besides, we can employ the optimized spiral waveguide [27] to reduce the transition loss in the long delay line in RAMZI. Second, an automatic control algorithm [26] including the thermal crosstalk needs to be further researched in the future to realize the accurate calibration and tuning. Third, we utilize three-stage structure to enlarge the extinction ratio, which increases the power consumption by hundreds of mW, compared with the two-stage structure. To solve this problem, we can employ other tuning methods with low energy consumption, such as the stress-optic phase tuner in the Si_3 N_4-based TriPleX platform [28]. Fourth, other resonator structures [29], with additional degrees of freedom compared to the employed all-pass microring on arms of the RAMZI, are alternative options to improve degrees of freedom of the spectral response reconstruction. Fifth, we can further double the FSR of the third stage, by setting the length difference of the MZI of the third stage to 0.5L, to enlarge the tuning range [18].

4. Conclusion

A rectangular optical lattice filter with a continuously tunable bandwidth and wavelength is proposed based on the zero-pole theory, and a Si_3N_4 photonic chip is fabricated to demonstrate the theory. The fabricated lattice filter shows a bandwidth tunability from 14.1 GHz to 4.1 GHz with a good rectangular response, and the center frequency can be tuned without changing the shape of the transmission response. The proposed structure is universally applicable and such a lattice filter with a tunable bandwidth and good shape factor can offer solutions to reconfigurable signal processing in optical communication networks and integrated microwave photonics.

Acknowledgment

The authors would like to thank LioniX B.V. for offering the TriPleX waveguide technology. The authors also would like to thank the anonymous reviewers for their valuable suggestions.

References

[1] S. Gringeri, B. Basch, V. Shukla, R. Egorov, and T. J. Xia, "Flexible architectures for optical transport nodes and networks," *Commun. Mag.*, vol. 48, no. 7, pp. 40–50, Jul. 2010.
[2] R. Dischler, F. Buchali, and A. Klekamp, "Demonstration of bit rate variable ROADM functionality on an optical OFDM superchannel," in *Optical. Fiber. Commun. Conf.*, 2010, Paper OTuM7.
[3] E. Pincemin *et al.*, "Multi-band OFDM transmission at 100 Gbps with sub-band optical switching," *J. Lightw. Technol.*, vol. 32, no. 12, pp. 2202–2219, Jun. 2014.
[4] D. Marpaung, C. Roeloffzen, R. Heideman, A. Leinse, S. Sales, and J. Capmany, "Integrated microwave photonics," *Laser Photon. Rev.*, vol. 7, no. 4, pp. 506–538, 2013.
[5] G. Poulopoulos *et al.*, "Fully flexible filtering element on SOI with 7-80 GHz bandwidth tunability and full FSR tuning," in *Proc. Opt. Fiber Commun. Conf. Expo.*, 2018, Paper M4H.6.
[6] T. Dai *et al.*, "Bandwidth tunable filter with large bandwidth and wavelength tuning range," in *Proc. Opt. Fiber Commun. Conf.*, 2018, Paper M4H.5.
[7] J. C. C. Mak, A. Bois, and J. K. S. Poon, "Programmable multi-ring butterworth filters with automated resonance and coupling tuning," in *Proc. Opt. Fiber Commun. Conf.*, 2016, Paper Tu2F.4.

[8] M. S. Rasras *et al.*, "Demonstration of a fourth-order pole-zero optical filter integrated using cmos processes," *J. Lightw. Technol.*, vol. 25, no. 1, pp. 87–92, Jan. 2007.
[9] P. Alipour *et al.*, "Fully reconfigurable compact RF photonic filters using high-q silicon microdisk resonators," *Opt. Express*, vol. 19, no. 17, pp. 15 899–15 907, Aug. 2011.
[10] P. Orlandi, F. Morichetti, M. J. Strain, M. Sorel, P. Bassi, and A. Melloni, "Photonic integrated filter with widely tunable bandwidth," *J. Lightw. Technol.*, vol. 32, no. 5, pp. 897–907, Mar. 2014.
[11] Y. Ding *et al.*, "Bandwidth and wavelength-tunable optical bandpass filter based on silicon microring-MZI structure," *Opt. Express*, vol. 19, no. 7, pp. 6462–6470, Mar. 2011.
[12] S. Djordjevic *et al.*, "Fully reconfigurable silicon photonic lattice filters with four cascaded unit cells," *IEEE Photon. Technol. Lett.*, vol. 23, no. 1, pp. 42–44, Jan. 2011.
[13] M. T. Boroojerdi, M. Ménard, and A. G. Kirk, "Wavelength tunable integrated add-drop filter with 10.6 nm bandwidth adjustability," *Opt. Express*, vol. 24, no. 19, pp. 22 043–22 050, Sep. 2016.
[14] Y. Stern *et al.*, "Tunable sharp and highly selective microwave-photonic band-pass filters based on stimulated brillouin scattering," *Photon. Res.*, vol. 2, no. 4, pp. B18–B25, Aug. 2014.
[15] K. Tanizawa, K. Suzuki, K. Ikeda, S. Namiki, and H. Kawashima, "Silicon photonic bandwidth-tunable filter based on 16-tap finite impulse response," in *Proc. Conf. Lasers Electro-Opt. Pacific Rim*, 2017, Paper s1097.
[16] Z. Wang, S.-J. Chang, C.-Y. Ni, and Y. J. Chen, "A high-performance ultracompact optical interleaver based on double-ring assisted Mach-Zehnder interferometer," *IEEE Photon. Technol. Lett.*, vol. 19, no. 14, pp. 1072–1074, Jul. 2007.
[17] H. Yu, M. Chen, P. Li, S. Yang, H. Chen, and S. Xie, "Silicon-on-insulator narrow-passband filter based on cascaded MZIs incorporating enhanced FSR for downconverting analog photonic links," *Opt. Express*, vol. 21, no. 6, pp. 6749–6755, Mar. 2013.
[18] M. C. Horton and R. J. Wenzel, "The digital elliptic filter–A compact sharp-cutoff design for wide bandstop or bandpass requirements," *IEEE Trans. Microw. Theory Techn.*, vol. 15, no. 5, pp. 307–314, May 1967.
[19] L. Zhuang, W. Beeker, A. Leinse, R. Heideman, P. van Dijk, and C. Roeloffzen, "Novel wideband microwave polarization network using a fully-reconfigurable photonic waveguide interleaver with a two-ring resonator-assisted asymmetric mach-zehnder structure," *Opt. Express*, vol. 21, no. 3, pp. 3114–3124, Feb. 2013.
[20] C. J. Kaalund and G.-D. Peng, "Pole-zero diagram approach to the design of ring resonator-based filters for photonic applications," *J. Lightw. Technol.*, vol. 22, no. 6, pp. 1548–1559, Jun. 2004.
[21] S. Darmawan, Y. M. Landobasa, and M.-K. Chin, "Pole–zero dynamics of high-order ring resonator filters," *J. Lightw. Technol.*, vol. 25, no. 6, pp. 1568–1575, Jun. 2007.
[22] C. K. Madsen and J. Zhao, *Optical Filter Design and Analysis: A Signal Processing Approach*, 1st ed. New York, NY, USA: Wiley, 1999.
[23] D. Baez-Lopez and T. Escalante, "Matlab based analog filter design," in *Proc. 29th Annu. Frontiers. Educ. Conf. Designing. the Future. of Science. and Engineering. Education. Conf. Proc.*, 1999, vol. 3, p. 13B4/1.
[24] C. Roeloffzen *et al.*, "Low loss si3n4 triplex optical waveguides: Technology and applications overview," *IEEE J. Sel. Topics Quantum Electron.*, vol. 24, no. 4, Jul./Aug. 2018, Art. no. 4400321.
[25] J. Li, Z. Liu, Q. Geng, S. Yang, H. Chen, and M. Chen, "Method for suppressing the frequency drift of integrated microwave photonic filters," *Opt. Express*, vol. 27, no. 23, pp. 33 575–33 585, Nov. 2019.
[26] S. S. Yegnanarayanan, R. T. Maxson, C. Sorace-Agaskar, D. Kharas, G. Steinbrecher, and P. W. Juodawlkis, "Automated initialization of reconfigurable silicon-nitride (sinx) filters," in *Proc. Conf. Lasers Electro-Opt.*, 2018, Paper JTh3D.4.
[27] T. Chen, H. Lee, and K. J. Vahala, "Design and characterization of whispering-gallery spiral waveguides," *Opt. Express*, vol. 22, no. 5, pp. 5196–5208, Mar. 2014.
[28] N. Hosseini *et al.*, "Stress-optic modulator in triplex platform using a piezoelectric lead zirconate titanate (PZT) thin film," *Opt. Express*, vol. 23, no. 11, pp. 14 018–14 026, Jun. 2015.
[29] M. G. Saber *et al.*, "Transversely coupled fabry-perot resonators with bragg grating reflectors," *Opt. Lett.*, vol. 43, no. 1, pp. 13–16, Jan. 2018.